Journal of Raman Spectroscopy

WILEY

Journal of RAMAN SPECTROSCOPY

RESEARCH ARTICLE OPEN ACCESS

Preparation and Identification of Heavy Minerals for Archaeometrical Studies: Villa of Fiumana (FC), Italy

S. Andò[1] | G. Vezzoli[1] | M. Barbarano[1] | L. Fornasini[2] | L. Saviane[3] | R. Villicich[3] | D. Bersani[2]

[1]Department of Earth and Environmental Sciences, DISAT, University of Milano-Bicocca, Milan, Italy | [2]Department of Mathematical, Physical and Computer Sciences, University of Parma, Parma, Italy | [3]Department of Humanities, Social Sciences and Cultural Industries, University of Parma, Parma, Italy

Correspondence: S. Andò (sergio.ando@unimib.it)

Received: 13 March 2025 | **Revised:** 26 July 2025 | **Accepted:** 1 August 2025

Funding: Funding was contributed by Project MIUR, Dipartimenti di Eccellenza 2023–2027, Department of Earth and Environmental Sciences, University of Milano-Bicocca.

Keywords: heavy-mineral | microscope | pottery | provenance | Raman spectroscopy

ABSTRACT

A new protocol for the laboratory preparation of archaeological samples, aimed at concentrating and analysing heavy minerals by optical microscope and Raman spectroscopy, is presented. The potential of heavy-mineral studies in geoarchaeology could be enhanced conspicuously by using a state-of-the-art protocol for sample preparation, analysing potteries, tempers and archaeological items, by high-resolution mineralogical analyses in medium silt and fine sand (15–250 μm). This method is repeatable by different operators, achievable in reasonable times, applicable also with a few grams of materials, and it is conceived to remove the abundant clayey and fine and very fine silt and liberate minerals from the ground mass. To test the proposed protocol, the mineralogical composition of 5 samples (common wares, red-painted ceramics and amphorae), collected in a Roman Villa sited in Fiumana, Forlì-Cesena, Italy, was investigated. The grain size analysed is representative (63%–75% in weight), and the amount of the 'heavy fraction' is very low (0.35%–0.72%), but sufficient to prepare a grain mount. Metamorphic versus magmatic minerals were quantified using a transmitted light, polarizing microscope, coupled with a Raman spectrometer and the presence of opaque and semi-opaque grains using an oblique light. This quantitative study allows us to differentiate samples that have been hand-crafted using different sediments as raw materials, discussing the source from the Alps and collected from the modern Po River depositional area; the sedimentary rocks of the Apennines; the volcanic source rocks from the Roman Province. This protocol is conceived to help improve the quality of heavy-mineral separation for applications in geoarchaeology.

1 | Introduction

The main component of the paste of most ceramics is clay [1], with common quartz grains, rock fragments and fragments of older ceramics. Clay minerals are too small to be analysed, with a single grain approach, by the polarizing light microscope and the use of Raman spectroscopy could not be considered a routine method identifying clay minerals and it is applied only in few studies [2]. Composition of archaeological ceramics is routinely analysed by thin section petrography [1] and by X-ray powder diffraction [3]. These studies are commonly focused on the bulk composition and texture of ceramics. Particulate inclusions are rarer, but they potentially contain a lot of petrographic information. Many sand tempers used for the fabrication of ceramics are sediments with heavy mineral contents that reflect the mineralogy of their source rocks [4]. The mineralogical composition of an archaeological fragment could represent a fingerprint and a proxy for reconstructing the geological and geographic provenance of the raw materials used to make tempers and other objects found in

archaeological sites [5, 6]. Heavy mineral techniques are powerful archaeometric tools to reveal the provenance of raw materials [7]. If the use of thin section is fundamental to describe the composition of ceramics, focusing the attention to three main components of a ceramics (the clay matrix, the particulate inclusions and the voids), the recent advances in the protocol of preparation of samples, coupled with the capacity to identify the composition of minerals and rock fragments by the use of Raman spectroscopy, suggest a new multidisciplinary approach for archaeological studies. In a provenance study information is obtained from the sedimentary record in order to ideally move back up from sink to source, reconstruct landscapes that no longer exist and reveal the forcing mechanisms of paleogeographic change. When we try to apply this approach in archaeology, our 'provenance study' (from the French provenir, 'to come from') represents the attempt to identify the source rock of the materials chosen for the preparation of ceramics. Each heavy mineral grain is a unique messenger of coded data, carrying the details of its ancestry and the vicissitudes of its sedimentary history [8]. A systematic provenance study with a multidisciplinary approach is recommended (using an optical microscope, coupled with a Raman spectrometer) as it allows you to get further information and to create a high-resolution dataset.

To test these ideas, the present study was focused on five archaeological samples from a multilayered site in Fiumana (Predappio, Forlì Cesena, Italy), including the ruins of an Urban-Rustic Villa. The site was first investigated by Giovanna Bermond Montanari in 1960 and 1962 [9]; then archaeological campaigns have restarted since 2022 [10]. Recent findings have confirmed and explored the previous investigations and what emerged from the satellite images acquired in 2021 and 2022. The site represents a settlement occupied since prehistoric and protohistoric ages, mostly in Roman times and Late Antiquity. At least two important building phases were identified: an early Imperial Urban-Rustic Villa and a late-antique Pavilions Villa. Both villas must have been prestigious houses, characterised by large spaces and luxurious furnishings and decorations. Materials of great variety were discovered: bricks, stones, marbles, coins (allowing the dating of specific layers), glasses, mortars, wall painting fragments and potteries. An archaeometric study on some of these pottery findings was recently performed through a dedicated laboratory protocol [11].

In the case of ceramics, it is possible to study the origin of the raw materials through the spectroscopic analysis of the assemblage of heavy minerals, after gravimetric separation. Raman spectroscopy permits identifying silt-sized grains down to the size of a few microns with the same precision level required in quantitative provenance analysis of sand-sized sediments [12].

2 | Geological and Structural Setting

The Apennines, an orogenic belt formed since the Late Oligocene, are the result of the subduction of the Adriatic plate beneath the European plate. This process led to rapid slab rollback and back-arc spreading in the western Mediterranean [13–15]. The Apennines comprise a single deep foredeep, the Po basin, characterised by a steeper monocline, accelerated subsidence rates and a high sediment supply [16, 17]. These factors are controlled by the interplay between tectonic, climatic and sedimentary processes, which were significantly accelerated during the onset of major Alpine glaciations (0.87 Ma) [18]. At a regional scale, the Northern Apennine and the Po basin are divided into several tectonic domains and units (Figure 1) [19, 20] and references therein.

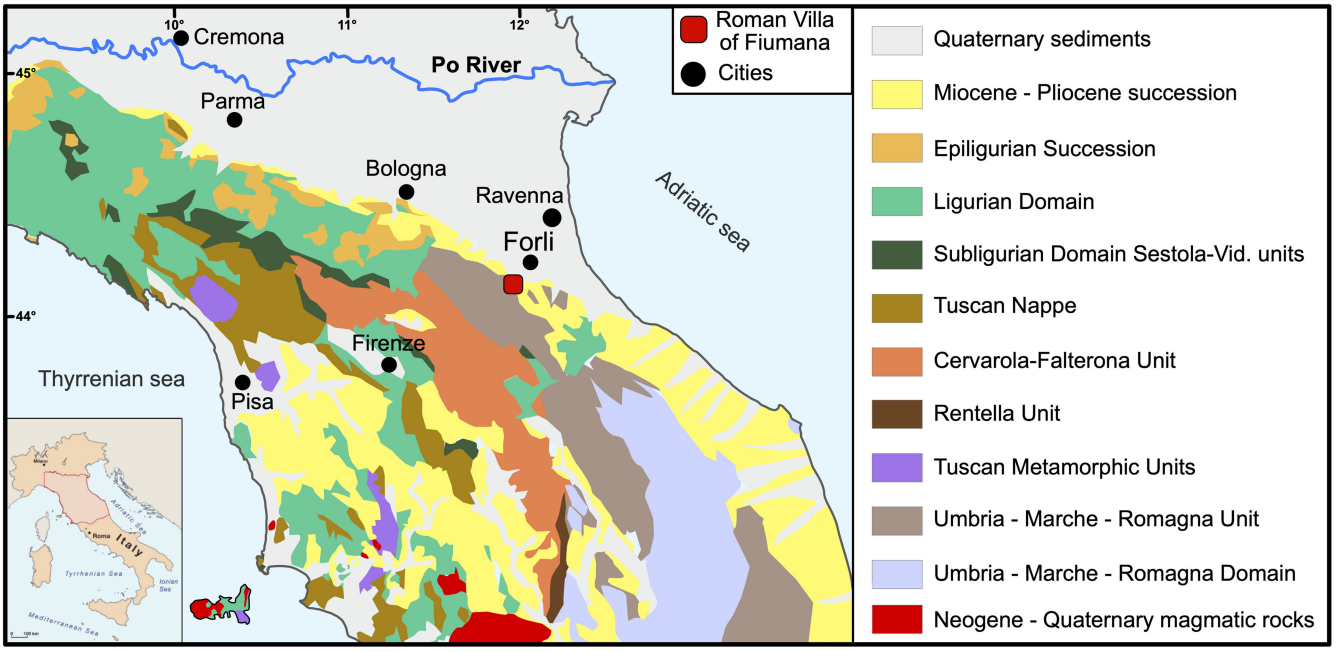

FIGURE 1 | Geological map of Northern Apennines with tectonic domains and outcrops of main lithologies. The site of the Roman Villa of Fiumana and main cities are shown.

2.1 | Quaternary Sediments

Quaternary alluvial and coastal deposits (e.g., conglomerates and sands) [21, 22] are widespread in the Po Basin, along the Tyrrhenian and Adriatic coastlines. In particular, the Po Basin was a Pliocene marine gulf between the Alps and the Apennines and gradually filled from west to east by Pleistocene alpine fluvial sediments [18].

2.2 | Miocene–Pliocene Succession

These succession records the depositional systems developed during the Messinian evaporite crisis [23]. Messinian sediments include salt deposits in the marginal areas and by pre-evaporite euxinic shales or siliciclastic turbidites in the basinal areas. The Pliocene marine deposits signify a pivotal phase in the Mediterranean Sea's history, marking its reconnection with the Atlantic Ocean following the Messinian crisis. This reconnection occurred through rapid and catastrophic marine ingression from the Gibraltar Strait. This is evident in the transgressive marine basal Pliocene clay deposits found in the back-arc of the Northern Apennines and other Mediterranean regions (e.g., [24, 25] with references therein).

2.3 | The Epiligurian Succession

The Epiligurian Succession was deposited within minor basins that were subsequently placed onto the Ligurian thrust sheets (the uppermost part of the orogenic wedge) [26]. This arrangement allowed for the configuration of the basins as satellite basins, thrust-top basins, wedge-top basins or piggy-back basins [27, 28]. These units are characterised by terrigenous rocks, bioclastic calcarenites, shallow marine marls and clayey marls, evaporite gypsum and bituminous muds.

2.4 | The Ligurian Domain

This domain encompasses magmatic–sedimentary successions that constitute the remnants of the Piedmont-Ligurian Ocean, as documented by Elter [29]. The Ligurian units were extensively buried by detritus eroded from the Alps and exhumed during the Plio-Quaternary periods [30]. These units are characterised by the presence of a basal ophiolite sequence, layered gabbro, thick Upper Cretaceous carbonate flysch deposits (Helminthoid Flysch) overlain by underlying associated sedimentary melanges [31, 32].

2.5 | The Subligurian Domain

The Subligurian Domain is usually thought to be in a paleogeographic position between the Ligurian and Tuscan Domains. The stratigraphic succession of the Subligurian Domain is marked by a prominent regional unconformity, dating back to the middle–late Eocene. This unconformity separates two distinct geological formations: (a) a pre-middle–late Eocene succession, spanning from the early Paleocene to the lower part of the middle Eocene; (b) A post-Eocene succession, comprising the earliest Oligocene and the earliest Miocene [33]. These units are characterised by a diverse range of sedimentary rocks, including shales, siltstones, limestones, and siliciclastic turbidite sandstones.

2.6 | Sestola-Vidiciatico Units

This tectonic mélange (early middle Miocene) comprises highly sheared rocks, interpreted as remnants of the subduction channel between the Ligurian prism and the Adriatic Plate [34]. The Sestola-Vidiciatico units are composed of juxtaposed tectonic slivers of various rock types that have been detached from both the overlying Ligurian units and the underlying Tuscan Successions.

2.7 | Tuscan Nappe

The sedimentary succession begins in the Triassic and continues until the Lower Jurassic with carbonate rocks (marine platform). Later, the Sinemurian extensional tectonics, coupled with the opening of the central Atlantic, resulted in the downthrowing of the carbonate shelf and in the pelagic sedimentation below the CCD. This pelagic environment endured throughout the Cretaceous and a segment of the Palaeogene periods, concurrently with the persistent subsidence of the seabed. Starting in the late Oligocene, turbidite sedimentation characterises the foredeep basin (Macigno Formation) until the early Miocene, when the stratigraphic cycle ceases due to the deposition of the overlying Ligurian Units [35, 36].

2.8 | The Cervarola-Falterona Unit

This sedimentary sequence was deposited in the outermost region of the Tuscan Domain and comprises lower marlstones, shales and limestones dating back to the pre-foredeep phase. It also includes a thick sandstone turbidite complex from the foredeep sedimentation phase. Finally, the upper marlstones and shales are associated with the basin closure phase [27, 35]. The Monte Cervarola Sandstones comprise turbidite sandstones and siltstones, constituting a thick succession characterised by a siliciclastic composition. The uppermost and younger portions of this unit exhibit a progressive increase in carbonate sandstone content [37].

2.9 | Rentella Unit

This unit lies between the Tuscan units and the Umbria-Marche-Romagna units [38]. The Rentella Succession is characterised by marlstones and siltstones (Rupelian-Aquitanian). Upward, the sequence changes to turbiditic marls (Aquitanian to Burdigalian [39]).

2.10 | Tuscan Metamorphic Units

Metamorphic rocks are indicative of the metamorphic processes that have occurred on the Tuscan margin of the Adria Plate.

They exhibit a Mesozoic–Cenozoic succession that is comparable to the Tuscan Nappe, as well as its underlying Palaeozoic basement. The metamorphic conditions are generally in the green schist facies, and high-pressure metamorphic rocks are only reported from scattered outcrops in central-southern Tuscany [40–42].

2.11 | Umbria-Marche-Romagna Unit

This succession is deposited in foreland basins, including simple foredeep and complex foredeep basins [39, 43]. These sedimentary rocks are mostly turbidites, with some starved euxinic shales and resedimented evaporites. Within the siliciclastic units, the Marnoso-arenacea Formation is predominantly represented. This formation comprises a remarkably thick turbidite complex that extends from the Emilia Apennines to the Umbria-Marche Apennines, spanning several hundred kilometres (e.g., [27, 35, 44].

2.12 | Umbria-Marche-Romagna Domain: Triassic-Miocene Units

In the Umbria-Marche-Romagna Apennines crops out extensively a thick and articulated sedimentary main succession deposited onto the more external sector of the Adria plate, subdivided in some minor successions [39, 43]. The Triassic-Lower Jurassic succession witnessed sedimentation in basins undergoing subsidence during this geological epoch. Consequently, the formation of extensive carbonate platform limestones occurred. Subsequently, the carbonate platform underwent fragmentation, resulting in a series of intrabasinal highs and lows. These geological features created diverse depositional environments that persisted throughout the Jurassic period. The Jurassic condensed succession, ranging from Sinemurian to Tithonian, was deposited on structural highs and consists of tidal massive limestones, followed by detrital facies [19]. The Cretaceous to Miocene units are initially distinguished by the Maiolica Formation, which signifies the termination of the predominant carbonate sedimentation within the Umbria-Marche Domain. The extensional events that previously impacted the carbonate platform cease, and uniform sedimentation conditions prevail throughout the basin [43]. Subsequently, the basin exhibits a gradual deepening, resulting in the deposition of micritic limestones interspersed with black chert layers and black pelites (e.g., Livello Selli and Livello Bonarelli; [45, 46]. Sedimentation persisted throughout the Cretaceous to Eocene periods. Notably, the Umbria-Marche Domain experienced shortening during the Miocene epoch, leading to its gradual transformation into a turbiditic foredeep.

2.13 | Neogene-Quaternary Magmatic Rocks

Neogene to Quaternary mafic to felsic volcanic rocks are found in the hinterland of the chain (Tuscany, Latium and small outcrops in Umbria [47]. Following tectonic phases characterised by shortening and nappe emplacement, concurrent with regional extension, magmatic activity occurred on the Tyrrhenian flank of the Apennine orogen. This geological process occurred during the Neogene and Quaternary epochs, resulting in the emplacement of plutonic, volcanic, and pyroclastic rocks. These rocks are now visible as outcrops in the Tuscan Archipelago, central and southern Tuscany and northern Latium [48].

3 | Archaeological Potteries From Villa di Fiumana

Different types of pottery fragments were discovered from Villa di Fiumana: kitchen pottery, common ware, red-painted ceramic and terra sigillata, amphorae and mortars. A recent investigation [11] was aimed at characterizing different types of pottery fragments, comparing the compositional, manufacturing and technological process through a multitechnique approach, combining optical microscopy, X-ray powder diffraction and micro-Raman spectroscopy. Information about the nature of the original clays was obtained from fossil fragments and phases formed during the firing process (i.e., gehlenite and pyroxenes). Firing temperatures and atmospheres were investigated through the formation of further new phases (i.e., feldspars), the alteration of phyllosilicates (i.e., micas) and the distinction of iron oxides. The identification of some heavy minerals in the fragments (i.e., apatite and epidote) highlighted the possibility of investigating the provenance of the raw materials through a dedicated study with heavy minerals techniques, which were fully explored in the present work.

4 | Materials and Methods

The protocol for heavy mineral separation takes inspiration from the method developed by Andò [49] to separate heavy minerals in sediments and sedimentary rocks. The choice of the grain size window is important to avoid introducing a bias during the laboratory preparation [50], tending heavy minerals to concentrate in the fine tail of sediment sources for hydraulic sorting in the depositional environments [51]. The study of the suite of heavy minerals in fragments of potteries requires a few additional specific 'tricks' as concentrating these minerals over a wide grain size, ranging from medium silt to fine sand (15–250 μm). The method adopted is only mechanical, avoiding chemical dissolution, and the wide grain size range is conceived for both Raman and optical studies, preparing grain mounts with the Canada Balsam. This bonding resin (refractive index, $n = 1.54$) is preferred to the classic and more resistant epoxy resin (araldite). Indeed, in the Canada Balsam spectrum, intense vibrational modes in the 140–1200 cm^{-1} frequency region (where most of the diagnostic peaks are encountered when analysing detrital and authigenic minerals in sediments, sedimentary rocks and potteries) and in the OH region, centred at 3800 cm^{-1}, are absent and thus have a very low influence on the identification of the Raman spectrum of the analysed mineral embedded in the bonding resin.

4.1 | Sample Preparation

A large number of potsherds were found during the archaeological excavations at the site of Villa di Fiumana. Five different types of ceramic fragments were selected and analysed: one handle of an

amphora, three fragments of red-painted potteries (two walls and one base) and one rim of a common ware (Figure 2). They were first weighed and disaggregated in an agate mortar with water, using an agate pestle. It is important to apply vertical pressure, avoiding grinding and minimizing undue pulverisation. The use of deionised water is recommended to work in a safe environment, avoiding breathing dust during the preparation of samples, reducing the health risk and enhancing the effect of pressure applied by the pestle. A progressive disaggregation is achieved by continuously alternating crushing and sieving. A steel sieve with a mesh of 250 μm is used, with a bottom, to recover the passing material. Because clay-rich fragments are dominant, in this procedure, a disaggregation of all grains encountered in the fraction coarser than 250 μm is performed. The fraction <250 μm is stored in a plastic beaker labelled with the sample name, and excess water is removed by siphoning. A sieve with a tissue mesh of 15 μm is prepared [49] and used to remove the <15 μm fraction. A clean 15–250 μm grain size fraction is thus prepared and dried overnight in the oven at 60°C. The dried fraction is weighed in a 50-mL conic tube, and a gravimetric separation with sodium-polytungstate (SPT, set at 2.90 g/cm^3) is achieved in a centrifuge, applying a speed of 2500 rpm (rpm) for 3 min. The partial freezing method in liquid nitrogen is applied to recover the light and dense fractions in different paper filters. The heavy and light mineral fractions are weighed, and a concentration of dense grains in the 15–250 μm grain size fraction is calculated. An aliquot of this fraction is micro-splitted with a handmade riffle box to minimize the effect of different grain sizes during splitting, obtaining a representative amount of HM (few milligrams) for each grain mount. Canada Balsam is melted at 130°C on a hot plate; on a regular glass slide for grain mounts, grains are poured and spread by a toothpick, and a square glass cover slip is gently placed and pressed to remove air bubbles to reduce the thickness of the mount. This easy and economical preparation may be considered one of the most appropriate to be analysed by optical microscope and Raman spectroscopy. Plastic boxes are also useful to prevent breaking the mounts and for storing the samples (Figure 3).

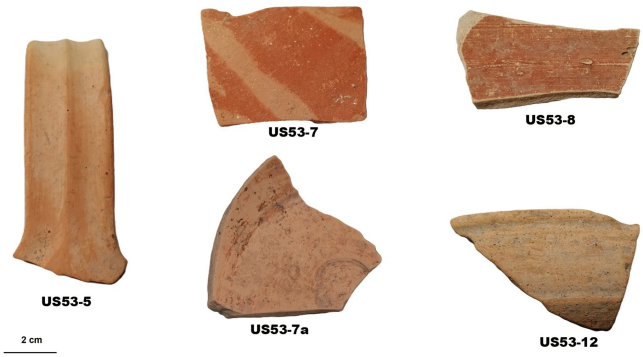

FIGURE 2 | Five different types of ceramics analysed in the archaeological site of Villa of Fiumana.

4.2 | High-Resolution Heavy Mineral Analysis

Raman spectroscopy has tremendous potential, serving as a fundamental complement to a variety of provenance methods including heavy-mineral analysis and bulk petrography. In particular, it represents a key tool for the characterisation of samples in archaeometrical studies [52–54]. Raman spectroscopy is an inelastic light-scattering technique widely used to study the vibrational properties of solids, liquids and gases [55, 56]. This approach has several advantages: (I) It is a user-friendly non-destructive technique; (II) it speeds the identification of different phases; (III) it has a micrometric resolution; (IV) samples routinely used for other optical methods are appropriate, and no time-consuming protocols are necessary to prepare the sample; (V) it can be used directly on rocks, HM slides and thin sections. The wide application of this method for detrital minerals identification has created the need for a calibrated database to compare unknown spectra with a certified standard [12]. The same method has triggered the publication of several papers to

FIGURE 3 | Heavy minerals encountered in the 15–250 μm grain size fraction (sample US53-5), shown in transmitted parallel light (TL) and reflected-oblique light plus two Nicol (RL) with Canada Balsam. The two methods are both necessary and complementary to identify the entire suite of dense grains. Heavy (HM) and light minerals (LM) dried and stored in plastic boxes after weighing. Grain mounts of a quartered aliquot of the heavy-mineral fractions for the five studied samples, prepared with Canada Balsam ($n = 1.56$) and labelled (in red, the rectangular areas analysed).

fill the gap and transform a qualitative approach into a more quantitative method [57–59]. Some disadvantages are still important, such as the low Raman signal of opaque minerals, the fluorescence and the presence of organic matter. A multimethod approach is required to give a proper name to each single grain. Raman spectroscopy is of paramount importance to identify dubious grains, weathered grains and variety of species in a group of minerals, but heavy-mineral suites in ceramics need to be observed also under transmitted and reflected light. The shape of each single grain, the surficial texture and the corrosion features are essential to quantify the effect of chemical dissolution [60]. The corrosion features of heavy minerals could be described under an optical microscope, using a standard protocol and the same magnification for the entire set of samples. In this study, the 20× objective is used for this aim, and it allows us to determine useful indices of corrosion to assess recycling and mechanical and chemical weathering. The oblique reflected light is a hybrid method, developed to identify opaque and semi-opaque heavy minerals, abundant or dominant in ceramics. The lack of significant recent literature and the bias introduced by the expertise of the operator is a weak point to be improved in the near future for a wider application of the suggested method.

4.3 | Heavy Mineral Counting

The counting of a representative aliquot of heavy grains is carried out after micro-quartering and mounting of HM on a glass slide with Canada balsam [49]. The choice of the counting method is also important to obtain a quantitative dataset, and different methods can be used. The choice depends on the type of sample analysed and the number of weathered grains. When oxides and hydroxides are dominant in the studied sample, to find a balance and to speed up the grain counting, the area method is applied [50, 61], choosing from two to four different areas in distant zones and randomly chosen on the entire surface of the slide. This approach is necessary when working with fragments of lithic artefacts, amphorae and ceramics, in which altered grains, opaque and semi-opaque iron oxides and hydroxides, and titanium oxides are always very abundant, and therefore, transparent HMs represent a minor part of the heavy grains mounted on the slide. The method allows obtaining a quantitative composition, considering all the types of grains encountered, showing the entire fingerprint of each sample. The choice of different sub-areas for counting all the grains present is close to what was proposed by Schönig et al. [62] for the suites of heavy minerals in modern sediments. It also allows applying the method in the archaeological field by balancing the amount of information obtained and the time needed to complete a count using the optical microscope and Raman spectroscopy. Such a thorough and high-resolution identification of the components that constitute the sample allows building a solid dataset to discuss and reconstruct the possible source rocks and the geographical areas of provenance of the raw materials used for the preparation of the ceramics. To implement this approach, Raman maps are prepared using a camera associated with a translation stage and Renishaw Wire 5.6 software and using a combination of transmitted light (low intensity) and oblique light (a commercial head-torch). These maps let one move around the slide and associate a description of the shape of the grain, a description of the optical properties and a Raman spectrum for each grain in

TABLE 1 | Results of gravimetric separation of heavy minerals in ceramics (after disaggregation and wet sieving at 15–250 μm). Light fraction < 2.90 g/cm^3; dense fraction > 2.90 g/cm^3.

Sample	Type of ceramic	Class analysed μm	Counting method	<15 μm	15–250 μm	>250 μm	% fine tail cut	% class analysed	Total sieved (g)	Total analysed (g)	Light fraction (g)	Dense fraction (g)	% HM/TOT
US53-5	Amphora handle	15–250	Area	4.542	7.776	0	37%	63%	12.318	7.776	7.748	0.028	0.35
US53-7	Common red painted pottery wall	15–250	Area	2.911	6.250	0	32%	68%	9.160	6.250	6.216	0.033	0.53
US53-7a	Common painted pottery base	15–250	Area	3.917	7.782	0	33%	67%	11.698	77.82	7.739	0.043	0.55
US53-8	Common painted pottery wall	15–250	Area	2.398	6.960	0	26%	74%	9.357	6.960	6.909	0.050	0.72
US53-12	Common pottery rim	15–250	Area	2.804	8.625	0	25%	75%	11.429	8.625	8.571	0.053	0.62

the analysed sub-area. All the grains in the counting area are then recognised under the microscope and grouped according to their optical properties into homogeneous groups which are given a descriptive name, shared and reproducible by different operators. The grains recognised under the microscope are then analysed under Raman spectroscope are thus given a name. The entire group identified by the optical properties will then have a name, as defined by the Raman identification. This approach takes care of accuracy but also considers time and speed of analysis. All the grains transparent in transmitted light are analysed by Raman spectroscopy. A category of transparent but strongly corroded grains, with low relief and isotropic, are identified, and a certain number of these are analysed by Raman spectroscopy to verify if they are a homogeneous category and what they are. Other categories are then introduced: semi-opaque grains with corroded and reddish surfaces (iron oxides and hydroxides); yellowish grains with granular and irregular outlines; brown-reddish biotite; clay fragments; granular titanium oxides. This approach allows obtaining fully characterised associations of minerals and heavy fragments, and an application of the 'microscope-Raman-microscope' recognition procedure allows retrospectively learning how to recognize the different components of the sample, a self-training that reduces the counting times of subsequent samples, limiting the use of Raman spectroscopy in future studies. Because of its accuracy, efficiency and versatility, the results of the Raman technique are indispensable for fully reliable identification of heavy minerals in grain mounts or thin sections [12]. Non-polarised micro-Raman spectra have been obtained for minerals in grain mounts embedded in Canada balsam. All the spectra are collected in a nearly backscattering geometry, with a Renishaw inVia spectrometer, equipped with a Leica DM2500 polarizing microscope and motorised x–y stages, using a 50× LWD (long working distance) objective, a solid-state 532-nm laser and a grating of 1800 lines/mm in the 140–1200 cm^{-1}. Acquisition time was ~30 s, spatial resolution < 5 μm, spectral resolution ± 1 cm^{-1} and power ≤ 10% for opaque and semi-opaque minerals and 50%–100% for transparent minerals (≤ 10 mW at the sample). Calibration was done

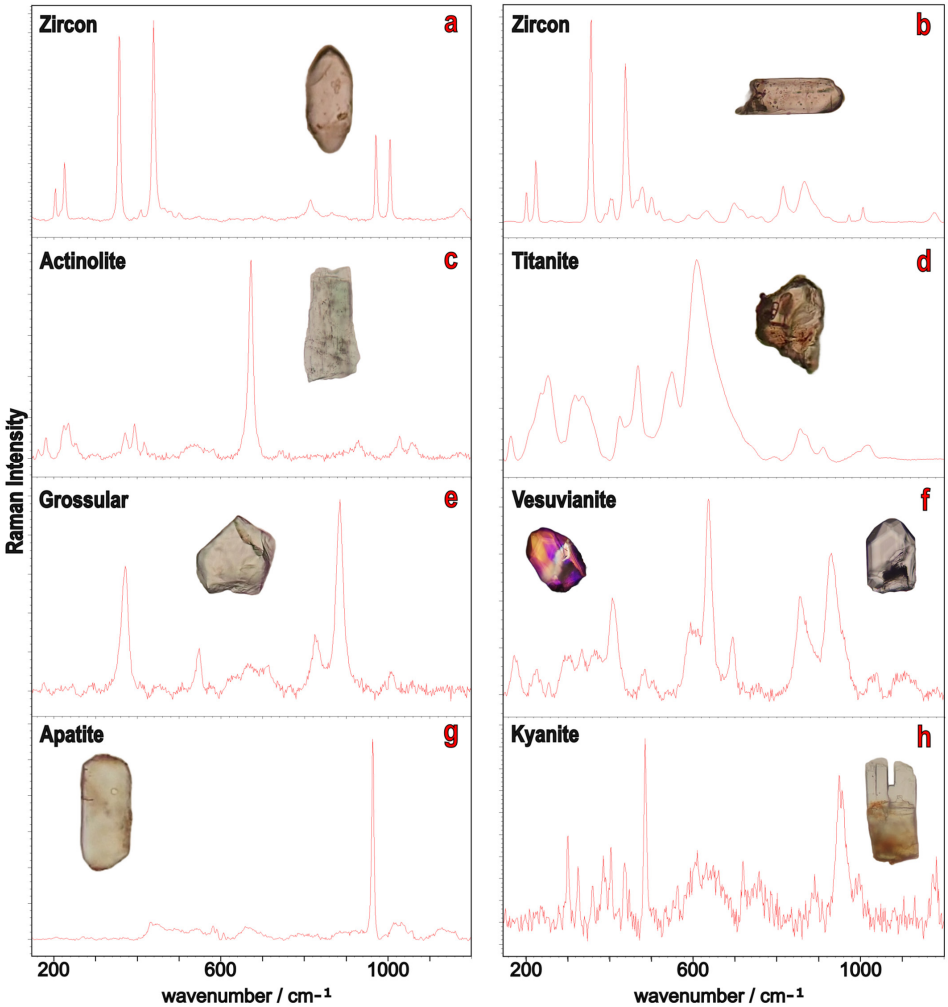

FIGURE 4 | Photos in transmitted light of different transparent heavy minerals encountered and identified in ceramics (15–250 μm grain size fraction), using the optical microscope and Raman spectroscopy. From top left to right: sharp euhedral prismatic crystal of zircon with the c-axis parallel to the direction of laser polarisation (a); broken prismatic crystal of zircon with the c-axis perpendicular to the direction of laser polarisation (b); prismatic actinolite with a pale bluish-green colour (c); irregular titanite with its typical high relief and dark rim (d); sharp irregular garnet (grossular) with conchoidal breakage pattern (e); euhedral crystal of vesuvianite, rich of faces (right, 1 Nicol), with anomalous interference tints, which range from deep yellow through purple to intense blue (left, two Nicol) (f); euhedral crystal of apatite with its distinctive low relief (g); prismatic kyanite exhibiting characteristic cross fractures and step-like features (h).

before each experimental session with a silicon wafer standard (peak at 520.5 cm^{-1}). A simple polynomial background subtraction was performed on each spectrum with Renishaw software (Wire 5.6) and the same program was used to perform spectral deconvolution, using Gauss–Lorentzian functions, to determine position, width and intensity of the Raman bands, and the Canada balsam spectrum has been very carefully subtracted from every spectrum presented.

5 | Results and Discussion

5.1 | Heavy-Mineral Data

Gravimetric separation of heavy minerals in ceramics was performed in the 15–250 μm grain size fraction starting from a determined aliquot (9 to 12 g per sample), which corresponds in size to about half of the fragments shown in (Figure 2). The analyzed granulometric class represents 63%–75% of the weight of the entire sample used. The dense fraction is always very low in weight with a relative amount of ~1%, and it is 0.4% in sample US53-5 and 0.5% in sample US53-7 (Table 1). Examples of single heavy minerals identified in ceramics are presented in Figures 4 and 5. The first optical observations acquired in transmitted light for different heavy minerals were confirmed using the optical microscope and Raman spectroscopy, focusing the laser on each single grain presented in these figures. A systematic and representative counting permits transforming the frequency into a percentage of different minerals. The terminology introduced by Garzanti and Andò [50] is applied to describe quantitatively the results of quantitative counting of different heavy minerals and to compare our data with previous analyses and references: very poor ($0.1 \leq tHMC < 0.5$), poor ($0.5 \leq tHMC < 1$), moderately poor ($1 \leq tHMC < 2$), moderately rich ($2 \leq tHMC < 5$), rich ($5 \leq tHMC < 10$), very rich ($10 \leq tHMC < 20$) or extremely rich ($tHMC > 20$). Following these criteria and classification, transparent heavy mineral concentration (tHMC) calculated in all samples after grain counting results very poor, ranging between 0.1% and 0.2% of transparent heavy minerals (authigenic, turbid and opaque heavy minerals are not considered in this calculation). The percentage of transparent detrital heavy minerals (tHM) varies in different samples (Table 2a). Taking advantage of the recent development in the capacity of identifying opaque and semi-opaque grains (osoHM) and because this could represent a quantitative approach for grouping different potteries, the relative percentage of transparent detrital minerals versus other types of grains encountered in this pilot study is considered (Table 2b). The highest values of tHM are measured in common red pottery wall sample US53-7 (56%) and in common pottery rim sample US53-12 (46%). The percentage of transparent detrital grains is (32%) in common painted pottery wall US53-8; (30%) in common painted pottery base US53-7a and (28%) in the amphora handle US53-5. Transparent metamorphic minerals are always encountered with epidote (3%–24%), garnet

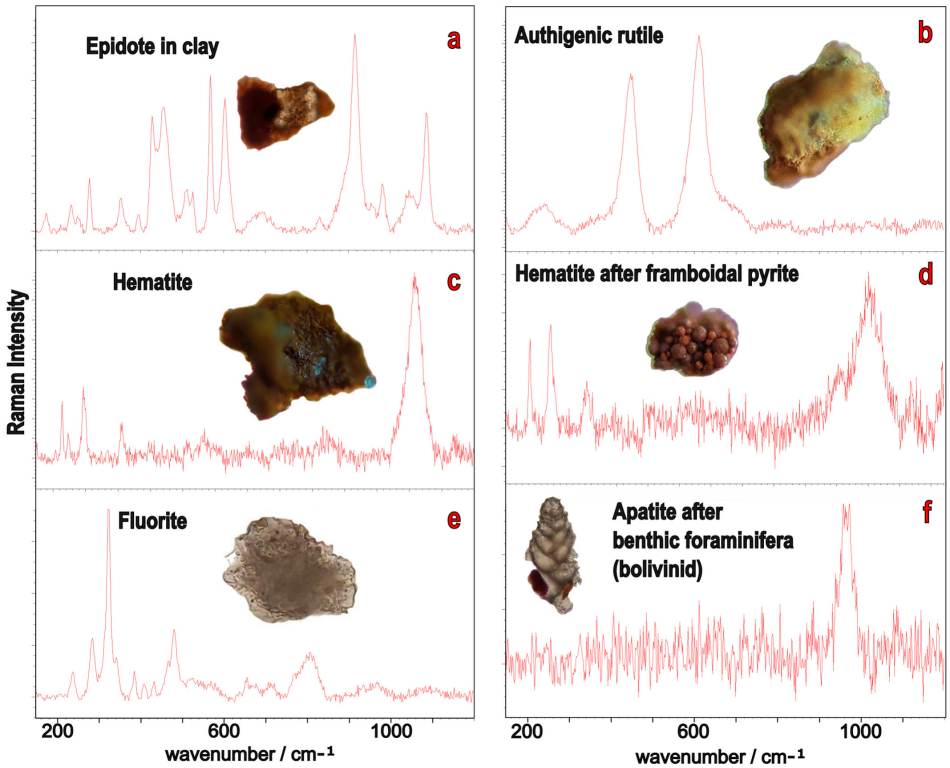

FIGURE 5 | Photos in transmitted and oblique reflected light of different opaque, semi-opaque and transparent heavy grains identified in ceramics (15–250 μm grain size fraction), using the optical microscope and Raman spectroscopy instrumentation. From top left to right: a brownish clay rich fragment with a stubby prism of yellowish-green epidote, exhibiting a fairly high relief and irregular shape (a); composite grain, identified as authigenic rutile, semi-opaque in transmitted light and yellowish in reflected light (b); angular and irregular brown and reddish secondary minerals, forming a mixture of hydrous ferric oxides and haematite (c); micrometric aggregates with spheroidal shape of haematite after framboidal pyrite, semi-opaque in transmitted light and reddish in reflected light (d); dusky and yellowish irregular fragment of fluorite with sharp edges (e); low crystallinity apatite after benthic foraminifer (bolivinid).

TABLE 2a | Quantitative heavy mineral data after point counting in grain mounts (15–250 μm). The HM percentage (in weight) calculated after the gravimetric separation is associated to each sample. The percentage of transparent heavy minerals and the percentage of all different heavy minerals encountered are indicated.

Sample	Type of ceramic	HM %weight	tHM %weight	Zircon	Dravite	Schorlite	Rutile	Titanite	Anatase	Brookite	Apatite	Monazite	Vesuvianite
US53-5	Amphora handle	0.21	0.06	15	0	0	5	14	1	0	42	1	1
US53-7	Common red painted pottery wall	0.22	0.12	13	0	0	12	34	1	0	27	1	0
US53-7a	Common painted pottery base	0.27	0.08	7	0	0	9	19	0	0	39	0.5	0
US53-8	Common painted pottery wall	0.21	0.07	24	0	0	7	20	2	0	38	0	0
US53-12	Common pottery rim	0.34	0.16	2	3	0.5	7	10	2	0.5	14	0	0

Sample	Type of ceramic	Oxy-hornblende	Tremolite	Actinolite	Diopside	Epidote	Clinozoisite	Other epidotes	Garnet	Staurolite	Kyanite	Total transparent
US53-5	Amphora handle	0	0	1	1	2	3	1	12	1	2	100
US53-7	Common red painted pottery wall	0	4	0	0	0	3	0	4	0	2	100
US53-7a	Common painted pottery base	0	0	0	0	7	2	0	14	0	2	100
US53-8	Common painted pottery wall	0	0	0.5	0	0	2	1	2	0	2	100
US53-12	Common pottery rim	0.5	0.5	0	0	14	10	0	37	0	0	100

TABLE 2b | Quantitative heavy mineral data after point counting in grain mounts (15–250 μm). The Zircon-Tourmaline-Rutile (ZTR) is associated with each sample. The relative percentage of transparent heavy minerals, opaque, and semi-opaque heavy minerals with hydroxides of iron and oxides of titanium (anatase and rutile) and fluorite are indicated. The relative percentage of HM, with rock fragments (RF), biotite and light minerals (light) are considered.

Sample	Type of ceramic	ZTR	% transparent	% opaque	% Fe Ox	% Ti Ox	% fluorite	Total	% HM	% RF	% biotite	% light	Total
US53-5	Amphora handle	20	28%	1%	39%	1%	31%	100%	60%	17%	23%	0%	100%
US53-7	Common red painted pottery wall	24	56%	2%	23%	8%	12%	100%	40%	23%	36%	1%	100%
US53-7a	Common painted pottery base	17	30%	2%	66%	2%	0%	100%	48%	28%	24%	0%	100%
US53-8	Common painted pottery wall	31	32%	15%	38%	15%	0%	100%	29%	46%	25%	0%	100%
US53-12	Common pottery rim	13	46%	1%	38%	15%	0%	100%	55%	22%	23%	0%	100%

(2%–37%), kyanite (0%–2%), trace of staurolite and amphiboles (0%–4%). Apatite is quite common (14%–42%) as well as titanite (10%–34%). Zircon is found (2%–24%) with detrital rutile (5%–12%). Tourmaline is rare, and 4% is encountered only in sample US53-12. Other rare minerals, such as clinopyroxene, monazite and vesuvianite, are also present in trace (Figure 5). Opaque minerals (e.g., magnetite) are always moderately poor (1%–2%), but they increase in sample US53-8 up to 15%. Fe-oxides and hydroxides are always extremely rich (23%–39%), and they represent (66%) in the common painted pottery base US53-7a. Ti-oxides are moderately poor (1%–2%) in samples US53-5 and US53-7a, respectively, rich (8%) in sample US53-7 and very rich (15%) in samples US53-8 and US53-12. Observation by oblique reflected light of different opaque and semi-opaque heavy grains is also important to quantify their relative amounts. Framboidal pyrite partially oxidised, which is common in sedimentary marine rocks formed in anoxic environments, is found. It is possible to distinguish red and yellow iron hydroxides, mainly goethite and white and yellow authigenic titanium oxides, respectively, authigenic granular anatase and rutile. Fluorite is encountered in the amphora handle U53-5 (31%) and in the common red painted pottery wall US53-7 (12%) always as corroded grains [28] (Figure 5).

6 | Conclusions

The small amount of material analysed in the potteries is proven to be enough to describe the entire suite of minerals and suggest that this method could be applied routinely in archaeological studies of ceramics and potteries, so abundant in each site of the analysed Roman Villa. Clinopyroxene is the most abundant non-opaque heavy mineral in nearly all tempers of volcanic derivation [63], and a suite with hornblende, epidote, garnets and Al-silicates represents a fingerprint for a sediment dominated by metamorphic source rocks, derived from orogenic settings. The average percentage in weight of transparent heavy minerals in the modern sediments of the Po River is 11%, and the typical composition of HM displays 77% of tHM, 12% opaque, 11% semi-opaque and the HM suite contains Zircon-Tourmaline-Rutile (3%), Titanite (2%), minerals from the epidote group (33%), garnet (31%), Al-silicates (3%), amphiboles (22%) and pyroxenes (7%) [64]. The average percentage in weight of transparent heavy minerals in sedimentary rocks from the Apennines is 2%, with 59% of tHM, 9% opaque and 33% semi-opaque. The HM suite shows Zircon-Tourmaline-Rutile (5%), Titanite (3%), epidote group minerals (17%), garnet (35%) and Al-silicates (3%), with a significant amount of amphiboles (14%) and pyroxenes (22%) and rare spinel (2%). In Gandolfi et al. [65], the heavy mineral suite was calculated in a different grain size window (63–250 μm). This study presents, in the northwestern part of the Marnoso-Arenacea and in the Macigno, a post-depositional loss of unstable heavy mineral species, with a dissolution of amphiboles, pyroxenes and epidotes due to intrastratal dissolution [65]. Orogenic minerals from the Alps, such as garnet, epidote and minor staurolite and kyanite, are recycled from extensively exposed foredeep turbidites [66, 67]. The comparison of data collected through time and in different laboratories with specific protocols introduces a bias. In our samples, the content of garnets is always lower than that encountered in the

sedimentary rocks studied in the Apennines, and we think this is a granulometric effect because garnets concentrate in the coarser sand fraction. The average amount of transparent HM is also lower because the heating vitrifies clay minerals, creating brown reddish weathering and patinas on detrital minerals. In this study of potteries, any mineral contained in sediments derived from the volcanic Roman Province is detected. Because a volcanic source providing common clinopyroxenes is thus excluded, suggesting the analysed potteries were not prepared with sediments collected near Rome, a different source is needed. The low concentration of heavy minerals and the high concentration of ultrastable minerals, such as zircon, rutile and tourmaline, combined with the absence of amphibole and pyroxene, suggests us that the modern sand of the Po River is not a possible source of the raw materials. The heavy mineral composition displays abundant metamorphic minerals with rare amphiboles and negligible metamorphic pyroxenes. This composition is more similar to the one observed by Gandolfi et al. [65] in the Marnoso-Arenacea Formation. It seems possible that samples have been handcrafted using, as raw materials, sediments derived from local sources, such as sediments deposited by rivers draining the sedimentary rock of the Apennines. The presence of fluorite suggests a possible additional source area of raw material in the Italian Prealps, as the village of Dossena (BG), where this mineral is known since the Roman period [68]. The Dossena-Gorno District (BG) was the only major zinc source in continental Italy, and it is this source that is probably also referred to by Pliny the Elder, who states clearly that a lapis aerosus called cadmea was exploited in this area [68, 69]. Ancient zinc and lead mining in Roman times were important for the production of brass, a gold-coloured copper-zinc alloy; rare tiny laminae are encountered in our sample containing fluorite. It is difficult to trace these minerals in potteries, and additional studies are necessary to prove this connection. It is interesting that the new proposed method suggests a new possible interpretation and fingerprint not detected with previous classical methods. The conscious use of fluorite in the preparation of pottery and the connection of people living in the study area with people in the Southern Alps, working in small ore sites to extract different minerals for the preparation of brass and fluorite, is of interest to explain the use of different types of raw materials in preparing different types of ceramics.

Acknowledgements

Eduardo Garzanti is warmly thanked for providing his encyclopaedic knowledge of the key references for the provenance of sediments in the Alps and Apennines. This work benefited through the years from numerous fruitful discussions with, and precious advice from, Claudia Conti and Peter Vandenabeele. Stimulating reviews by Roberta Somma and Dorota Salata are gratefully acknowledged. Funding was contributed by Project MIUR, Dipartimenti di Eccellenza 2023–2027, Department of Earth and Environmental Sciences, University of Milano-Bicocca. Open access publishing facilitated by Universita degli Studi di Milano-Bicocca, as part of the Wiley - CRUI-CARE agreement.

Conflicts of Interest

The authors declare no conflicts of interest.

Data Availability Statement

The data that support the findings of this study are available from the corresponding author upon reasonable request.

References

1. P. S. Quinn, *Ceramic Petrography—The interpretation of Archaeological Pottery & Related Artefacts in Thin Section* (Archaeopress, 2013): 251.

2. U. Villanueva, J. C. Raposo, K. Castro, A. de Diego, G. Arana, and J. M. Madariaga, "Raman Spectroscopy Speciation of Natural and Anthropogenic Solid Phases in River and Estuarine Sediments With Appreciable Amount of Clay and Organic Matter," *Journal of Raman Spectroscopy* 39 (2008): 1195–1203.

3. V. Guarino, A. De Bonis, C. Grifa, A. Longella, V. Morra, and L. Pedroni, "Archaeometric Study on Terra Sigillata From Cales (Italy)," *Periodico di Mineralogia* 80, no. 3 (2011): 455–470.

4. U. Zimmermann, E. S. Kristoffersen, P. D. Fredriksen, S. A. R. Bertolino, S. Andò, and D. Bersani, "Provenance and Composition of Unusually Chrome and Nickel-Rich Bucket-Shaped Pottery From Rogaland (Southwestern Norway)," *Sedimentary Geology* 336 (2016): 183–196.

5. B. Borgers, G. Tol, and T. de Haas, "Roman Cooking Vessels (Ollae): A Preliminary Study of the Material From the Pontine Region, Central Italy," *Science and Technology of Archaeological Research* 3, no. 2 (2017): 314–325.

6. F. Bernardini, D. Lenaz, J. Horvat, A. Bavdek, P. Ventura, and A. De Min, "Provenance of Late Republican Roman Pottery From Caput Adriae Revealed by Non-Invasive Mineral Chemistry of Melanitic Garnets and Other Igneous Minerals," *Periodico di Mineralogia* 90 (2021): 29–43.

7. M. A. Mange and T. Bezeczky, "The Provenance of Paste and Temper in Roman Amphorae From the Istrian Peninsula, Croatia," in *Heavy Minerals in Use; Developments in Sedimentology Series, 40*, vol. 58, eds. M. A. Mange and D. T. Wright (Elsevier, 2007): 1007–1033.

8. M. A. Mange and D. T. Wright, "Introduction and Overview," in *Heavy Minerals in Use; Developments in Sedimentology Series*, vol. 58, eds. M. A. Mange and D. T. Wright (Elsevier, 2007): xxvii.

9. G.B. Montanari, "La Villa Romana di Fiumana", from: La villa romana. Giornata di studi, Russi 10 maggio 1970, Faenza, (1971): 51–73.

10. R. Villicich, A. Morigi, M. Gregori, L. Saviane, and E. Gardini, "La Villa di Fiumana (Forlì)," in *Abitare nel Mediterraneo Tardoantico*". Atti del IV Convegno Internazionale del Centro Interuniversitario di Studi sull'Edilizia abitativa tardoantica nel Mediterraneo (Cuenca, 7–9 novembre 2022), Bari, eds. I. Baldini, C. Sfameni, and M. Á. Valero Tévar (EDIPUGLIA, 2024): 21–32.

11. L. Saviane, "Nuove Ricerche Archeologiche a Fiumana (Predappio, FC). Saggi Stratigrafici Nell'area del Padiglione Occidentale e Indagini Archeometriche su Alcuni Materiali Rinvenuti", Master's Degree Thesis, Università di Parma, 2023/2024, (2024).

12. S. Andò and E. Garzanti, "Raman Spectroscopy in Heavy-Mineral Studies," in *Sediment Provenance Studies in Hydrocarbon Exploration and Production, Special Publications*, eds. R. A. Scott, H. R. Smyth, A. C. Morton, and N. Richardson (Geological Society, 2013): 395–412.

13. C. Faccenna, C. Piromallo, A. Crespo-Blanc, L. Jolivet, and F. Rossetti, "Lateral Slab Deformation and the Origin of the Western Mediterranean Arcs," *Tectonics* 23, no. 1 (2004): TC1012.

14. C. Doglioni, E. Carminati, M. Cuffaro, and D. Scrocca, "Subduction Kinematics and Dynamic Constraints," *Earth-Science Reviews* 83, no. 3–4 (2007): 125–175.

15. G. Molli, "Northern Apennine–Corsica Orogenic System: An Updated Overview," *Geological Society of London* 298, no. 1 (2008): 413–442.

16. M. Pieri and G. Groppi, "Subsurface Geological Structure of the Po Plain, Italy," *Progetto Finalizzato Geodinamica* 414 (1981): 1–13.

17. C. Doglioni, P. Harabaglia, S. Merlini, F. Mongelli, A. T. Peccerillo, and C. Piromallo, "Orogens and Slabs vs. Their Direction of Subduction," *Earth-Science Reviews* 45, no. 3–4 (1999): 167–208.

18. G. Muttoni, C. Carcano, E. Garzanti, et al., "Onset of Major Pleistocene Glaciations in the Alps," *Geology* 31, no. 11 (2003): 989–992.

19. P. Conti, G. Cornamusini, and L. Carmignani, "An Outline of the Geology of the Northern Apennines (Italy), With Geological Map at 1:250.000 Scale," *Italian Journal of Geosciences* 139, no. 2 (2020): 149–194.

20. E. Garzanti, G. Vezzoli, and S. Andò, "Paleogeographic and Paleodrainage Changes During Pleistocene Glaciations (Po Plain, Northern Italy)," *Earth-Science Reviews* 105, no. 1–2 (2011): 25–48.

21. A. Amorosi, V. Rossi, G. Sarti, and R. Mattei, "Coalescent Valley Fills From the Late Quaternary Record of Tuscany (Italy)," *Quaternary International* 288 (2013): 129–138.

22. M. Ghinassi, "Chute Channels in the Holocene High-Sinuosity River Deposits of the Firenze Plain, Tuscany, Italy," *Sedimentology* 58, no. 3 (2011): 618–642.

23. M. Roveri, S. Lugli, and V. Manzi, "The Desiccation and Catastrophic Refilling of the Mediterranean: 50 Years of Facts, Hypotheses, and Myths Around the Messinian Salinity Crisis," *Annual Review of Marine Science* 17 (2024): 485–509.

24. M. Ghielmi, M. Minervini, C. Nini, S. Rogledi, and M. Rossi, "Late Miocene–Middle Pleistocene Sequences in the Po Plain–Northern Adriatic Sea (Italy): The Stratigraphic Record of Modification Phases Affecting a Complex Foreland Basin," *Marine and Petroleum Geology* 42 (2013): 50–81.

25. F. Riforgiato, L. M. Foresi, A. Di Stefano, et al., "The Miocene/Pliocene Boundary in the Mediterranean Area: New Insights From a High-Resolution Micropalaeontological and Cyclostratigraphical Study (Cava Serredi Section, Central Italy)," *Palaeogeography, Palaeoclimatology, Palaeoecology* 305, no. 1–4 (2011): 310–328.

26. H. Wittmann, M. G. Malusà, A. Resentini, E. Garzanti, and S. Niedermann, "The Cosmogenic Record of Mountain Erosion Transmitted Across a Foreland Basin: Source-to-Sink Analysis of In Situ 10Be, 26Al and 21Ne in Sediment of the Po River Catchment," *Earth and Planetary Science Letters* 452 (2016): 258–271.

27. A. Argnani and F. Ricci Lucchi, "Tertiary Silicoclastic Turbidite Systems of the Northern Apennines," in *Anatomy of an Orogen: the Apennines and Adjacent Mediterranean Basins*, eds. G. B. Vai and I. P. Martini (Kluwer Academic Publisherluwer Academic Publisher, 2001): 327–350.

28. G. G. Ori and P. F. Friend, "Sedimentary Basins Formed and Carried Piggyback on Active Thrust Sheets," *Geology* 12 (1984): 475–478.

29. P. Elter, "L'ensemble Ligure," *Bulletin de la Société Géologique de France* 17 (1975): 984–997.

30. M. G. Malusà and M. L. Balestrieri, "Burial and Exhumation Across the Alps-Apennines Junction Zone Constrained by Fission-Track Analysis on Modern River Sands," *Terra Nova* 24, no. 3 (2012): 221–226.

31. L. Cortesogno, B. Galbiati, and G. Principi, "Note alla Carta Geologica Delle Ofioliti del Bracco e Ricostruzione Della Paleogeografia Giurassico-Cretacica," *Ofioliti* 12 (1987): 261–342.

32. M. Marroni, G. Molli, G. Ottria, and P. Pandolfi, "Tectono Sedimentary Evolution of the External Liguride units (Northern Apennines, Italy): Insights in the Pre-Collisional History of a Fossil Ocean-Continent Transition Zone," *Geodinamica Acta* 14 (2001): 307–320.

33. P. Vannucchi, F. Remitti, and G. Bettelli, "Lateral Variability of the Erosive Plate Boundary in the Northern Apennines, Italy," *Italian Journal of Geosciences* 131, no. 2 (2012): 215–227.

34. P. Vannucchi, F. Remitti, and G. Bettelli, "Geological Record of Fluid Flow and Seismogenesis Along an Erosive Subducting Plate Boundary," *Nature* 451, no. 7179 (2008): 699–703.

35. F. Ricci Lucchi, "The Oligocene to Recent Foreland Basins of the Northern Apennines," in *Foreland Basins, International Association of Sedimentologists*, vol. 8, eds. P. A. Allen and P. Homewood (Special Publications, 1986): 105–139.

36. M. Fazzuoli, G. Ferrini, E. Pandeli, and G. Sguazzoni, "Le Formazioni Giurassico-Mioceniche Della Falda Toscana a Nord Dell'Arno: Considerazioni Sull'evoluzione Sedimentaria," *Memorie della Societa Geologica Italiana* 30 (1985): 159–201.

37. R. Tinterri and A. Piazza, "Turbidites Facies Response to the Morphological Confinement of a Foredeep (Cervarola Sandstones Formation, Miocene, Northern Apennines, Italy)," *Sedimentology* 66 (2019): 636–674.

38. F. Brozzetti, L. Luchetti, and G. Pialli, "La Successione del Monte Rentella (Umbria Occidentale); Biostratigrafia a Nannofossili Calcarei ed Ipotesi per un Inquadramento Tettonico Regionale," *Bollettino della Societa Geologica Italiana* 119, no. 2 (2000): 407–422.

39. M. Barchi and M. Marroni, *Note Illustrative Della Carta Geologica d'Italia Alla Scala 1:50.000 "Foglio 310—Passignano sul Trasimeno"* (Servizio Geologico d'Italia, 2014): 196.

40. G. Molli, A. Vitale Brovarone, O. Beyssac, and I. Cinquini, "RSCM Thermometry in the Alpi Apuane (NW Tuscany, Italy): New Contraints for the Metamorphic and Tectonic History of the Inner Northern Apennines," *Journal of Structural Geology* 113 (2018): 200–216.

41. M. Franceschelli, G. Gianelli, E. Pandeli, and M. Puxeddu, "Variscan and Alpine Metamorphic Events in the Northern Apennines (Italy): A Review," *Periodico di Mineralogia* 73, no. 2 (2004): 43–56.

42. F. Rossetti, C. Faccenna, L. Jolivet, B. Goffé, and R. Funiciello, "Structural Signature and Exhumation P–T–t Paths of the Blueschist Units Exposed in the Interior of the Northern Apennine Chain, Tectonic Implication," *Bollettino della Societa Geologica Italiana* 1 (2002): 829–842.

43. M. Barchi, A. Landuzzi, G. Minelli, and G. Pialli, "Outer Northern Apennines," in *Anatomy of an Orogen, The Apennines and Adjacent Mediterranean Basins*, eds. G. B. Vai and I. P. Martini (Kluver Academic Publisher, 2001): 215–254.

44. A. Tagliaferri and R. Tinterri, "The Tectonically-Confined Firenzuola Turbidite System (Marnoso-Arenacea Formation, Northern Apennines, Italy)," *Italian Journal of Geosciences* 135, no. 3 (2016): 425–443.

45. G. Bonarelli, *1901, "Descrizione Geologica Dell'Umbria Centrale" (Opera Postuma Curata per Incarico del Centro Umbro di Studi per le Risorse Energetiche)* da: C. Lippi-Boncambi, R. Signorini, C. Giovagnotti, C. Alimenti, M. Alimenti. Poligrafica F. Salvati, (1967), pp. 156.

46. S. R. Meyers, S. E. Siewert, B. S. Singer, et al., "Intercalibration of Radioisotopic and Astrochronologic Time Scales for the Cenomanian-Turonian Boundary Interval, Western Interior Basin, USA," *Geology* 40, no. 1 (2012): 7–10.

47. I. Innocenti, G. Serri, G. Ferrara, P. Manetti, and S. Tonarini, "Genesis and Classification of the Rocks of the Tuscan Magmatic Province: Thirty Years After Marinelli's Model," *Acta Vulcanologica* 2 (1992): 247–265.

48. A. Peccerillo and M. L. Frezzotti, "Magmatism, Mantle Evolution and Geodynamics at the Converging Plate Margins of Italy," *Journal of the Geological Society of London* 172, no. 4 (2015): 407–427.

49. S. Andò, "Gravimetric Separation of Heavy Minerals in Sediments and Rocks," *Minerals* 10 (2020): 273.

50. E. Garzanti and S. Andò, "Heavy Minerals for Junior Woodchucks," *Minerals* 9 (2019): 148.

51. E. Garzanti, S. Andò, and G. Vezzoli, "Grain-Size Dependence of Sediment Composition and Environmental Bias in Provenance Studies," *Earth and Planetary Science Letters* 277 (2009): 422–432.

52. P. Vandenabeele, H. G. M. Edwards, and L. Moens, "A Decade of Raman Spectroscopy in Art and Archaeology," *Chemical Reviews* 107, no. 3 (2007): 675–686.

53. D. Bersani and P. P. Lottici, "Raman Spectroscopy of Minerals and Mineral Pigments in Archaeometry," *Journal of Raman Spectroscopy* 47 (2016): 499–530.

54. A. Rousaki, L. Moens, and P. Vandenabeele, "Archaeological Investigations (Archaeometry)," *Physical Sciences Reviews* 20170048 (2018): 1–9.

55. P. F. McMillan, "Raman Spectroscopy in Mineralogy and Geochemistry," *Annual Review of Earth and Planetary Sciences* 17 (1989): 255–279.

56. L. Nasdala, D. Smith, R. Kaindl, and M. Ziemann, "Raman Spectroscopy: Analytical Perspectives in Mineralogical Research," *EMU Notes in Mineralogy* 1, no. 12 (2004): 281–343.

57. D. Bersani, S. Andò, P. Vignola, et al., "Micro-Raman Spectroscopy as a Routine Tool for Garnet Analysis," *Spectrochimica Acta Part A: Molecular and Biomolecular Spectroscopy* 73, no. 3 (2009): 484–491.

58. D. Bersani, S. Andò, L. Scrocco, et al., "Composition of Amphiboles in the Tremolite–Ferro–Actinolite Series by Raman Spectroscopy," *Minerals* 9, no. 8 (2019): 491.

59. L. Borromeo, S. Andò, D. Bersani, et al., "Detrital Orthopyroxene as a Tracer of Geodynamic Setting: A Raman and SEM-EDS Provenance Study," *Chemical Geology* 596 (2022): 120809.

60. S. Andò, E. Garzanti, M. Padoan, and M. Limonta, "Corrosion of Heavy Minerals During Weathering and Diagenesis: A Catalog for Optical Analysis," *Sedimentary Geology* 280 (2012): 165–178.

61. J. S. Galehouse, "Counting Grain Mounts; Number Percentage vs. Number Frequency," *Journal of Sedimentary Research* 39, no. 2 (1969): 812–815.

62. J. Schönig, "Heavy-Mineral Grain Counting: Counting Techniques, Error Estimation, and the Number of Grains to be Counted," *Journal of Geophysical Research: Earth Surface* 129 (2024): e2023JF007337.

63. R. Dickinson William, "Discriminating Among Volcanic Temper Sands in Prehistoric Potsherds of Pacific Oceania Using Heavy Minerals," in *Heavy Minerals in Use; Developments in Sedimentology Series, 39*, vol. 58, eds. M. A. Mange and D. T. Wright (Elsevier, 2007): 985.

64. E. Garzanti and S. Andò, "Chapter 29, Plate Tectonics and Heavy Mineral Suites of Modern Sands," in *Heavy Minerals in Use, Developments in Sedimentology Series*, vol. 58 (Elsevier, 2007): 741–763.

65. G. Gandolfi, L. Paganelli, and G. G. Zuffa, "Petrology and Dispersal Pattern in the Marnoso-Arenacea Formation (Miocene, Northern Apennines)," *Journal of Sedimentary Petrology* 53, no. 2 (1983): 493–507.

66. E. Garzanti, S. Canclini, F. M. Foggia, and N. Petrella, "Unraveling Magmatic and Orogenic Provenance in Modern Sand: The Back-Arc Side of the Apennine Thrust Belt, Italy," *Journal of Sedimentary Research* 72, no. 1 (2002): 2–17.

67. E. Garzanti and M. G. Malusà, "The Oligocene Alps: Domal Unroofing and Drainage Development During Early Orogenic Growth," *Earth and Planetary Science Letters* 268 (2008): 487–500.

68. A. Maass, A. Celauro, and S. Merkel, "... nunc et in Bergomatium agro ... The Zinc Mining Area in the Dossena-Gorno District Near Bergamo as a Possible Source for Roman Brass", Conference paper. In Bèla Török and Alessandra Giumlia-Mair; *Proceedings of the 5th International Conference Archaeometallurgy in Europe*, 73, (2021): 303–328.

69. H. Rackham, trans. *Pliny Natural History*, Volume IX, Books XXXIII–XXXV, (Cambridge, 1934).